Orientation effects in H_2 dissociation by He^{2+} impact at $v_P=1$ and 2 a.u.

S. Martínez,* G. Bernardi, P. Focke, D. Fregenal, and S. Suárez
Centro Atómico Bariloche and Instituto Balseiro, Comisión Nacional de Energía Atómica and Universidad Nacional de Cuyo, 8400 San Carlos de Bariloche, Río Negro, Argentina
(Received 2 September 2005; published 30 December 2005)

We have investigated the dependence of two electron processes leading to dissociation on the orientation of the H_2 molecule, by measuring differential cross sections for proton fragment emission in coincidence with the outgoing projectile charge state. Proton energy spectra (4–15 eV) emerging at angles 10° and 90° were obtained for He^+ and He^0 charge states from $He^{2+}+H_2$ collisions at $E_P=25$ and 100 keV/amu ($v_P=1$ and 2 a.u.). By means of the Franck-Condon approximation we found the contribution to the proton emission from the $2p\pi_u$, $2s\sigma_g$, $2p\sigma_u$, and Coulomb explosion dissociation channels, allowing us to obtain cross sections for double capture, transfer ionization, and transfer excitation processes. Cross sections for double ionization and ionization plus excitation were also obtained from the measured data. The results were discussed on the basis of a two-step model within the independent electron approximation, using a perturbative approach for the single capture process.

DOI: 10.1103/PhysRevA.72.062722 PACS number(s): 34.50.Gb, 34.70.+e, 34.90.+q

I. INTRODUCTION

Research in ion-molecule collisions is relevant for the understanding of many processes in astronomy, in the atmosphere physics, and in several application fields such as plasma physics and biology. These applications require mainly the knowledge of total cross-section data for the processes implied. Theoretical and experimental efforts have been devoted to the study of basic processes involved in collisions with molecular targets. The methods to treat a molecular target have been developed from those applied to ion-atom collisions, the multicenter nature being its main signature. In this sense, and compared to complex molecules, the simplest H_2 molecule serves as a test case, as atomic hydrogen does in ion-atom collisions.

Collisions of bare projectiles with H_2 give rise to numerous output channels, some of them leading to dissociation of the target. For our presently reported range of measurements, He^{2+} impact at $v_P=1$ a.u. and $v_P=2$ a.u., the dominant processes are nondissociative capture and nondissociative ionization, respectively. Among the two-electron processes, transfer ionization plays a significant role in this collision energy range. Considerable attention, both experimental and theoretical, has received charge transfer in H^+ and He^{2+} on H_2 collisions including the final (n,l) distribution of the captured electron. For the present energy range, model calculations based on perturbative approximations are close to their lower limit of validity, while close-coupling theory using atomic or molecular orbitals was successfully applied below 100 keV/amu. Also the classical trajectory Monte Carlo (CTMC) method, appropriate at intermediate impact energies, was used to study charge transfer in H_2.

In the intermediate- to high-energy collision range, charge transfer in H^+ on H_2 was calculated using the Born approximation by Tuan and Gerjuoy [1]. The same approximation, but within the impact parameter formalism, was applied by Wang *et al.* [2] and Deb *et al.* [3], in order to investigate the dependence of the capture cross section with the orientation of the molecule. Corchs *et al.* [4] and Busnengo *et al.* [5] performed calculations for H^+ and He^{2+} projectiles on H_2 using a distorted-wave formalism. From the preceding works, where the ground state of H_2 is expanded in terms of one-electron wave functions around each proton, the two-center character of the target is clearly displayed in the probability amplitude for single-electron capture as

$$a_M(\mathbf{b}) = a_A(\mathbf{b}_A) + a_B(\mathbf{b}_B)e^{i\delta}, \tag{1}$$

where the impact parameter $\mathbf{b}$ refers to the middle point of the internuclear molecular axis, and $\mathbf{b}_{A,B}$ are the impact parameters with respect to atomic centers A and B. The phase δ is given by $\delta=\alpha_z\rho\cos\theta$, with $\boldsymbol{\alpha}=\mathbf{K}_f-\mathbf{K}_i$; $\mathbf{K}_i$, $\mathbf{K}_f$ are the initial and final momentum of the projectile moving in the z direction. Finally $\boldsymbol{\rho}$ is the H_2 internuclear vector, with an orientation given by the angle θ with respect to the projectile direction. In expression (1) the transition amplitude for the molecular target is expressed as a coherent sum of the atomic amplitudes $a_{A,B}$ for each atomic center, with a phase difference δ. This phase introduces an interference term in the one-electron capture probability $|a_M|^2$, which leads to a dependence of the cross section on the orientation of the internuclear axis of the molecule. Considering the more probable process in which the H_2^+ ion is left in a gerade state [1,2], constructive interference is obtained for $\delta=0$, i.e., the perpendicular orientation of the molecule. It must be noted that amplitude transitions in molecular targets can be expanded in a multicenter way if the electron wave functions are sufficiently localized around each center. Furthermore, it is expected that molecular orientation effects become noticeable when the typical impact parameter is not too large as compared to the internuclear distance of the molecule.

Extensive investigations of one and two-electron processes for the H_2 target were performed by Edwards and collaborators in the intermediate to high-energy impact re-

*Electronic address: smartine@cab.cnea.gov.ar

gime. Orientation dependence for two-electron removal in H_2 was measured with H^+, D^+, and He^+ projectiles [6]. Total cross sections for single and double ionization were also obtained [7–9]. Nagy and Végh [10,11] compared their theoretical results with these experimental data, and discussed the contributions of different mechanisms for two-electron transitions within a perturbative approximation. Orientation dependence of cross sections for double ionization, ionization plus excitation, and double excitation has been measured also by Edwards *et al.* [12] for H^+ on H_2 at 0.75-, 1-, and 2-MeV energy and for electron impact.

At the low to intermediate energy collision regime, Shingal and Lin [13] performed calculations for charge transfer with H^+ and He^{2+} on H_2, including the orientation dependence of the cross section. By using the expression (1) for the H_2 target, as obtained in a perturbative treatment, they calculated the atomic amplitudes with an atomic-orbital (AO) expansion model. After averaging over the orientation of the target internuclear axis, they found good agreement with experimental data for total charge-transfer cross section for both projectiles, particularly for incident energies up to 100 keV/amu. Charge transfer for the same collision system was studied by Fritsch [14,15] by means of a modified two-center atomic-orbital (AO+) model that resulted in a reasonable agreement with total cross-section measurements.

Meng *et al.* [16] applied the CTMC method to electron capture in He^{2+} on H_2 collisions, for different final $He^+(n,l)$ states, from $n=1$ to 6 and $l=0$, 1, and 2. Good agreement with their own experimental results and with total cross-section data from Shah and Gilbody [17] and Frieling *et al.* [18] was obtained at intermediate impact energy. Experimental results in state-selective capture for the same collision partners, for energies up to 25 keV/amu, were performed by Hoekstra *et al.* [19].

For incident projectiles with charges and energies out of the perturbative region, like in the present measurements, Cheng *et al.* [20] studied the system O^{8+} on D_2 for incident energies $E_P=2-16$ MeV. They observed a dependence on the orientation for the transfer ionization plus transfer excitation channel, while a near isotropic behavior is obtained for ionization plus excitation, including double ionization. To interpret the orientation dependence within an independent electron model, they assume that the alignment is due only to the electron-capture process [20,21]. A qualitative agreement with the experimental results is obtained by using expression (1) applied to single capture. At the same time, they argue that the continuous distributions of electron energies in an ionization processes, contained in the momentum transfer α_z in Eq. (1), lead to average out the interference effect, resulting in a nearly isotropic cross section. The orientation dependence of charge-transfer processes to specific n projectile states was also studied by Busnengo *et al.* [22] for O^{8+} on H_2 by applying a distorted-wave formalism.

More elaborated calculations, with the aim to assess the orientation dependence in transfer excitation processes, were performed with a two-step model in an independent electron approximation by Wang *et al.* [23] and Corchs *et al.* [24]. Transfer excitation probability is calculated as a product of the probabilities for the transfer and excitation processes, which are separately obtained as a function of the impact parameter. They found that both processes, single-electron transfer and excitation of the remaining H_2^+ ion, participate in the dependence of the cross section with molecular orientation. With this two-step model they obtained a better agreement with experimental results for transfer excitation in O^{8+} on H_2 [24].

Recently, this two center approach, expression (1), has been applied to interpret experimental results for single capture for He^{2+}, Ar^{2+}, and N^{2+} on H_2^+ or D_2^+, i.e., a true single active electron process without the ambiguity of a multielectron target [25,26]. Excellent agreement between experimental and theoretical results for total cross sections was obtained. For the alignment dependence, it was demonstrated that the perpendicular orientation is preferred, achieving a qualitative agreement with the experimental data.

In the present work, measurements for He^{2+} impact on H_2 are reported. We study the dissociative capture processes at 25- and 100-keV/amu collision energies and their dependence on the molecular target orientation. Doubly differential cross sections (DDCS) for proton fragments with energies between 4 and 15 eV and emission angles of $\theta=10°$ and 90°, relative to the beam direction, were obtained in coincidence with outgoing He^+ and He^0 projectiles. As usual in fast collisions measurements, we considered that the direction of the emitted proton is defined by the orientation of the hydrogen molecule axis at the time of the collision, allowing us to discuss the dependence of the measured processes with the molecular alignment. The analysis of the spectra, based on the Franck-Condon approximation, led us to find the contribution for double capture (DC), transfer ionization (TI), and transfer excitation (TE) processes:

$$He^{2+} + H_2 \rightarrow He^0 + 2H^+ \quad \text{DC}, \tag{2a}$$

$$He^{2+} + H_2 \rightarrow He^+ + 2H^+ + e^- \quad \text{TI}, \tag{2b}$$

$$He^{2+} + H_2 \rightarrow He^+ + H_2^{+*} \rightarrow He^+ + H^+ + H^0 \quad \text{TE}. \tag{2c}$$

Subtracting both coincidence spectra, i.e., with He^0 and He^+ outgoing projectiles, from the total proton emission, which was also measured, we were able to estimate the contributions from double ionization (DI) and ionization plus excitation (IE) processes:

$$He^{2+} + H_2 \rightarrow He^{2+} + 2H^+ + 2e^- \quad \text{DI}, \tag{3a}$$

$$He^{2+} + H_2 \rightarrow He^{2+} + H_2^{+*} + e^- \rightarrow He^{2+} + H^+ + H^0 + e^- \quad \text{IE}. \tag{3b}$$

Cross sections of excitation to the $2p\pi_u$, $2s\sigma_g$, $2p\sigma_u$ states with simultaneous capture (TE) and ionization (IE) were estimated from the data analysis.

II. EXPERIMENTAL PROCEDURE

Proton-fragment energy distributions were measured with an electrostatic analyzer, placed at selected emission angles, as described previously [27,28]. The gas target effuses from a microchannel array fixed at the tip of a 0.5-mm-diameter tube. As a more collimated flow is obtained compared to the

single tube used previously, the microchannel array was moved away from the ion beam and placed at a distance of 2 mm.

The beam is separated into its charge state components after exiting the collision chamber, by means of an electrostatic deflector. Neutral (He^0) and charged (He^+) projectiles are analyzed and detected by secondary emission conversion electrodes with electron multiplier devices [29]. The dissociative capture processes are identified by measuring coincidences between angle and energy analyzed proton fragments and He^+ and neutral He^0 outgoing projectiles. Total proton emission spectra were obtained in an independent set of measurements, with the same methods employed in a previous work [28]. The base pressure in the collision chamber was 7.0×10^{-8} Torr. Coincidence measurements were performed at a working pressure of 4.8×10^{-6} Torr with the effused H_2 target inside the chamber. Typical He^{2+} beam current, in total proton production (noncoincidence) measurements, was 10 pA. In the coincidence measurements the beam current was adjusted in order to obtain count rates of $6-8\times10^4$ counts/sec of He^+ and 4×10^4 counts/sec of He^0 at the projectile detectors.

Proton spectra were measured in the range 4–15 eV only at emission angles $\theta=10°$ and 90°, because the coincidence rates were very low. The effective target thickness dependence on the detection angle was estimated as described previously in Ref. [30]. The correction factors applied to the spectra were 0.68 at $\theta=10°$ and 1 at $\theta=90°$. In coincidence measurements we obtained the number of proton-He^+ or proton-He^0 coincidence events, simultaneously with the total number of protons (start pulses), both normalized to a fixed quantity of He^+ or He^0 counts in the corresponding ion detector (stop pulses). Then, besides dissociative capture data, a doubly differential distribution for total proton emission was obtained at the same time, for selected energies and emission angles. By achieving the best agreement between this total emission distribution and that obtained in noncoincidence condition, already normalized to absolute values [28], we get absolute cross-section values for the dissociative capture data. The efficiency of the coincidence system was estimated to be $(87\pm3)\%$ from additional measurements.

Double collision events and the contamination of charge state fractions other than He^{2+} in the incident beam must be considered as a source of experimental uncertainties. These processes could also result in the emission of a proton and an outgoing He^+ (He^0) ion in coincidence, then contributing mistakenly to the dissociative capture counting. For a diluted gas target the probability of double collision events is much smaller than that for a single collision. Moreover, one of the double collisions must be dissociative and yield protons with the proper measured energy, which makes this effect unlikely. An estimation of the contribution of double collision events to the processes of interest resulted in less than 1%. Charge state fractions of the incident beam were obtained by measuring the count rate from the projectile detector at the end of the beam line, 900 mm downstream of the target. Data were taken for three different configurations: (i) without gas target; (ii) with the target at the same pressure as that used during measurements; and (iii) with a uniform distribution of gas in the collision chamber at the same working pressure as (ii). Finally, the charge fractions of the incident beam on the target during coincidence measurements were found to be He^{2+}, 98.1%; He^+, 1.75%; He^0, 0.15% at 25 keV/amu and He^{2+}, 98.65%; He^+, 1.25%; He^0, 0.1% at 100 keV/amu. To estimate the effect of the contaminants He^+ and He^0 in the primary He^{2+} beam, we considered only single collision events leading to the same final products as those in a dissociative capture collision. These are dissociative capture and dissociative ionization of a target by a He^+ projectile (He^0 beam contamination is negligible). We conclude that the contribution to the coincidence counting from these contaminant is less than 3% for proton-He^0 and negligible for proton-He^+ events.

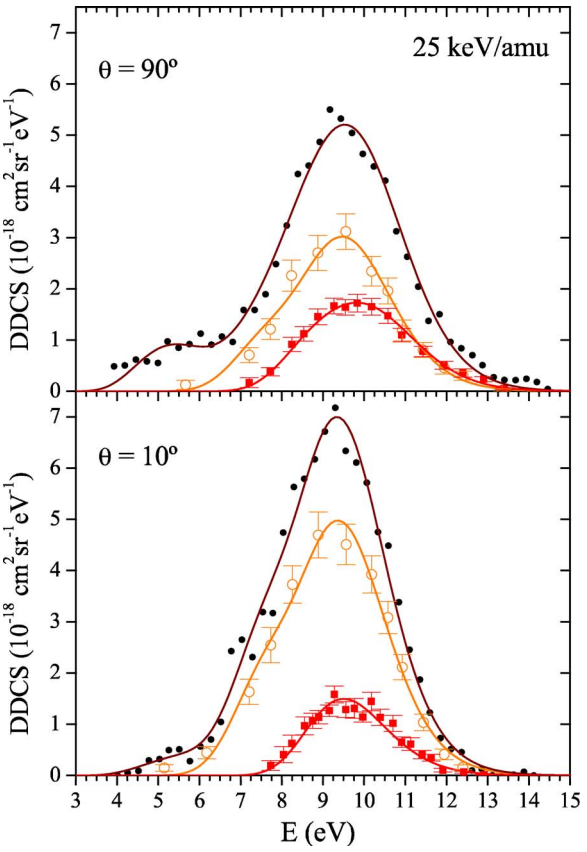

FIG. 1. (Color online) DDCS for proton emission in He^{2+} on H_2 at 25-keV/amu impact energy. (●) Total proton production, (○) proton-He^+ coincidences, and (■) proton-He^0 coincidences. The solid curves are fits to the data; see text. Error bars come from statistical uncertainties.

III. RESULTS AND DISCUSSION

The energy spectra of protons measured for 25 and 100 keV/amu are shown in Figs. 1 and 2, respectively. The total proton emission spectra (noncoincidence measurement), as well as those corresponding to proton-He^+ and proton-He^0 coincidences are displayed in absolute cross-section values. Evidently, the spectra of proton-He^0 coincidences correspond to DC process, reaction (2a), leading to Coulomb explosion (CE) of the two protons from H_2. In the case of the spectra for proton-He^+ coincidences, two possibilities arise, reac-

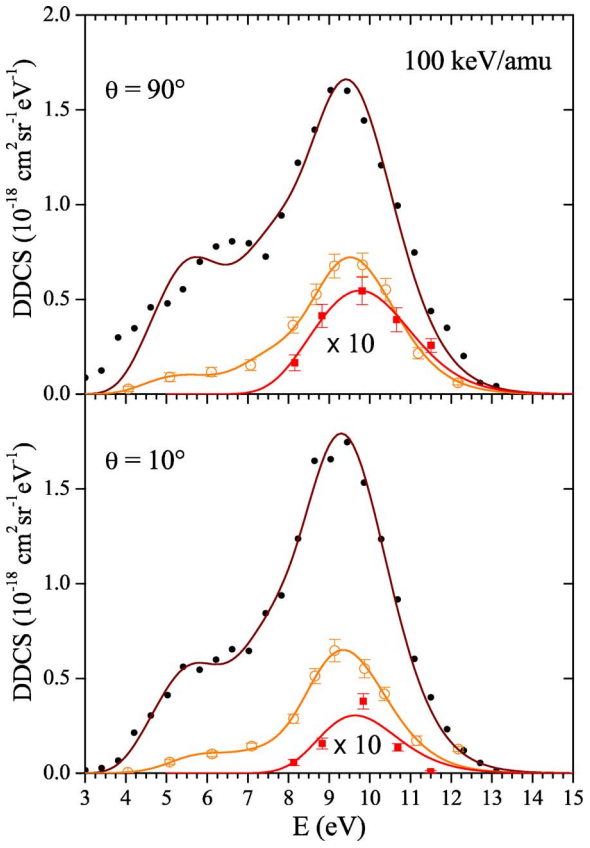

FIG. 2. (Color online) DDCS for proton emission in He^{2+} on H_2 at 100-keV/amu impact energy. (●) Total proton production, (○) proton-He^+ coincidences, and (■) proton-He^0 coincidences. (DC cross sections are enlarged by a factor of 10). The solid curves are fits to the data; see text. Error bars come from statistical uncertainties.

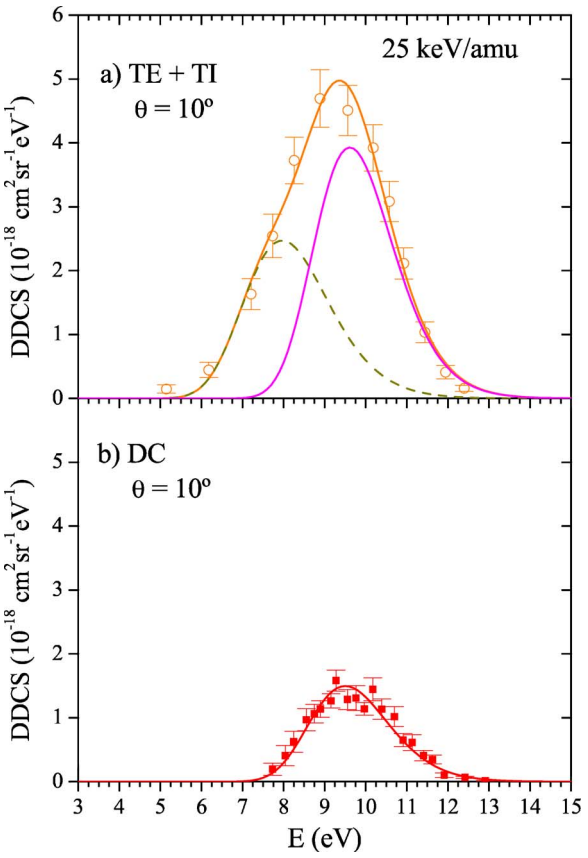

FIG. 3. (Color online) DDCS for proton emission in He^{2+} on H_2 at 25 keV/amu and emission angle θ=10°. (a) Transfer excitation plus transfer ionization, (b) double capture. Fitting curves of the dissociation channels are shown as follows: (—) CE, (- - -) transfer plus excitation to the $2p\sigma_u$ state.

tions (2b) and (2c). The TI process results again in CE, yielding protons with characteristic energy value determined by the initial internuclear distance of the hydrogen molecule. Also, single-electron capture can be accompanied by excitation of the remaining H_2^+ ion to dissociative states, leading to $H^+ + H(n,l)$ products. To analyze TE processes we considered $2p\pi_u$, $2s\sigma_g$, and $2p\sigma_u$ excited states. We should note that in a CE event any of the two protons can be detected, while in TE the detection of the emitted fragments is restricted to the charged one. Then, a factor of 2 must be taken into account in the proton yields for excited states in order to estimate cross-section values for TE processes.

The analysis of the spectra was done with the same method used previously [28]. Basically, we applied a fitting procedure with four components corresponding to the $2p\pi_u$, $2s\sigma_g$, $2p\sigma_u$, and CE repulsive states. Energy distributions of the emitted protons, for each dissociative state, were obtained within the Franck-Condon approximation and further broadened to include the effect of the translational thermal motion of the target molecules. As discussed previously [28], a subtle improvement in the fit of the experimental spectra is obtained by considering the collisional momentum transfer to the target. It is assumed that electronic transitions induced by the projectile are followed by molecule fragmentation, in two independent steps. In this way, the calculated distributions for proton emission can be transformed by considering the movement of the molecule center of mass. The uncertainties resulting from this procedure prevent us from using this method to determine momentum transfer from the experiment, although the momentum values obtained from the fitting procedure are close to the expected values, as resulted from energy and momentum conservation equations. We estimated the uncertainties in the yields from the fitting procedure including the uncertainty coming from the calibration of the energy axis. Typical values for DC were 15% (25 keV/amu) and 20% (100 keV/amu), 10% for TE and 5% for TI at both energies.

The results of the experimental data fitting are shown in Figs. 3 and 4 for 25 keV/amu, and in Figs. 5 and 6 for 100-keV/amu impact energies, respectively. The contribution to the total proton production from DI and IE were obtained by subtracting the fitting curves of the proton-He^0 and proton-He^+ coincidence spectra from the fitting of the total proton production spectra. In Figs. 7 and 8 we present the results corresponding to CE (DI) and contributions of the $2p\pi_u$, $2s\sigma_g$, and $2p\sigma_u$ states to IE. In the estimation of the uncertainties we included those coming from the fitting procedure, as well as the uncertainties in the yields of the total proton production and the coincidence data. In order to ob-

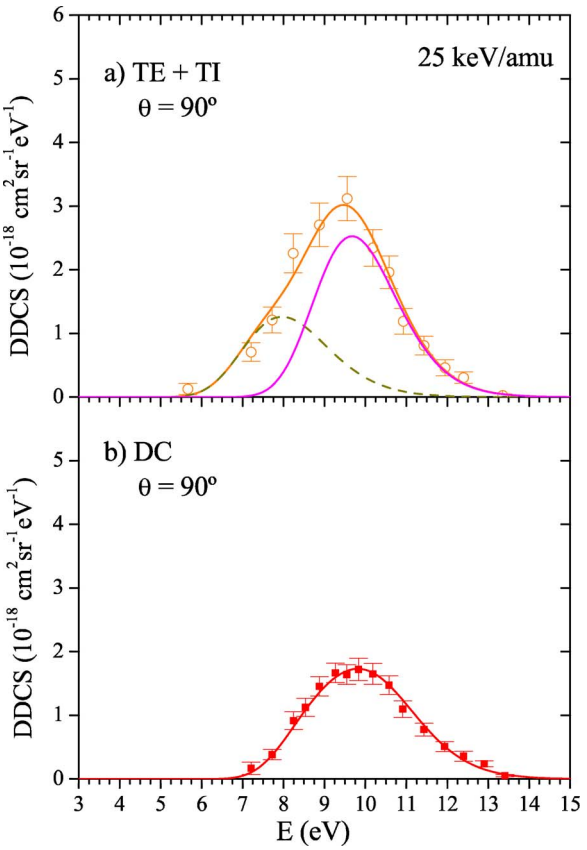

FIG. 4. (Color online) The same as in Fig. 3 for θ=90°.

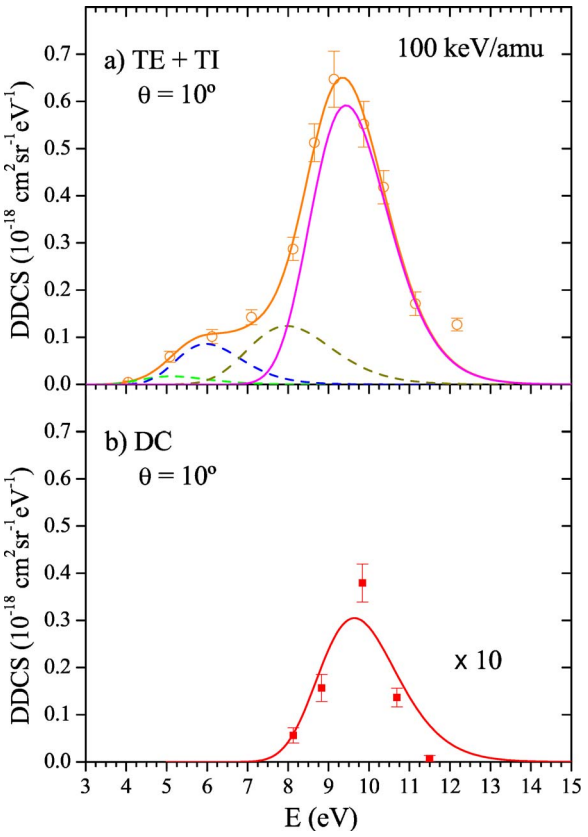

FIG. 5. (Color online) DDCS for proton emission in He^{2+} on H_2 at 100 keV/amu and emission angle θ=10°. (a) Transfer excitation plus transfer ionization, (b) double capture. Fitting curves of the dissociation channels are shown as follows: (—) CE, (- - -) transfer plus excitation (from lower to higher energies, $2p\pi_u$, $2s\sigma_g$, and $2p\sigma_u$ excited states).

tain differential cross sections $\sigma(\theta)=d\sigma/d(\cos\theta)$, as a function of emission angle θ, the energy integral of the different dissociative channels was calculated. The cross-section values were compiled in Tables I and II, where the uncertainties due to normalization to absolute values, as well as those derived from the fitting procedure, are included.

From the estimated cross-section data, it is clear that DC and TI processes are dominant in CE at 25 keV/amu, while DI has a small contribution. On the contrary, at 100 keV/amu, CE comes mainly from DI and TI, with a negligible DC contribution. These observations are in accordance with the trend of total cross sections [17,31,32] where transfer cross sections are higher than ionization cross sections at 25 keV/amu, and become lower at 100 keV/amu. In its turn, the TI contribution remains important at both energies. Excitation channels also showed a transition from a TE contribution larger than IE at 25 keV/amu, to an inverse behavior at 100 keV/amu impact energy.

For the purpose of displaying the dependence of the dissociation processes with the molecular orientation, the different cross sections are represented in polar coordinates in Figs. 9–11. It can be seen that DC is more likely for perpendicular molecular alignment (θ=90°) than for the near parallel one (θ=10°), for both incident energies. TI shows a preferred parallel orientation at 25 keV/amu and a near isotropic behavior at 100 keV/amu. DI has a preferred perpendicular orientation at 25 keV/amu, but the cross section is small and uncertainties are very large, while it turns out to be slightly parallel at 100 keV/amu. It is worth noting that CE, which is the sum of DC, TI, and DI, manifests an isotropic behavior for both impact energies (Fig. 9). If we consider TE, the only significant contribution at 25 keV/amu comes from the $2p\sigma_u$ state, with a clear parallel orientation. At 100 keV/amu the $2p\sigma_u$ state has, on the contrary, a perpendicular orientation. The same orientation is observed for the $2p\pi_u$ state, while in the case of the $2s\sigma_g$ state the large uncertainties prevent us from identifying the trend. For the total TE process at 100 keV/amu we observed a perpendicular orientation (Fig. 10). In the case of IE at 25 keV/amu the experimental uncertainties were large. Then, apart from the perpendicular orientation for the $2p\pi_u$ state (see Table I), the alignment dependence cannot be determined unambiguously. At 100 keV/amu, we observed an isotropic behavior for the states $2p\sigma_u$ and $2p\pi_u$. Within present uncertainties, a departure from an isotropic behavior for the $2s\sigma_g$ state cannot be asserted. For the total IE process the distributions are isotropic at both collision energies.

Two-electron processes have been extensively studied, particularly for the He target [33–35]. Several mechanisms have been proposed in order to interpret the experimental results, some relying on electron correlation, as the so-called shake process. In a shake mechanism one electron is ionized or captured by an interaction with the projectile, and then a second electron is promoted to excited (shake-up) or con-

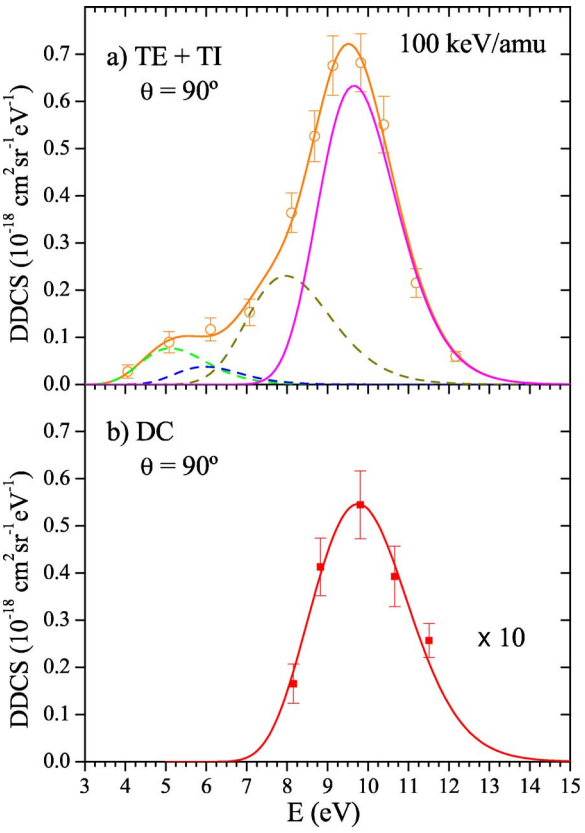

FIG. 6. (Color online) The same as in Fig. 5 for θ=90°.

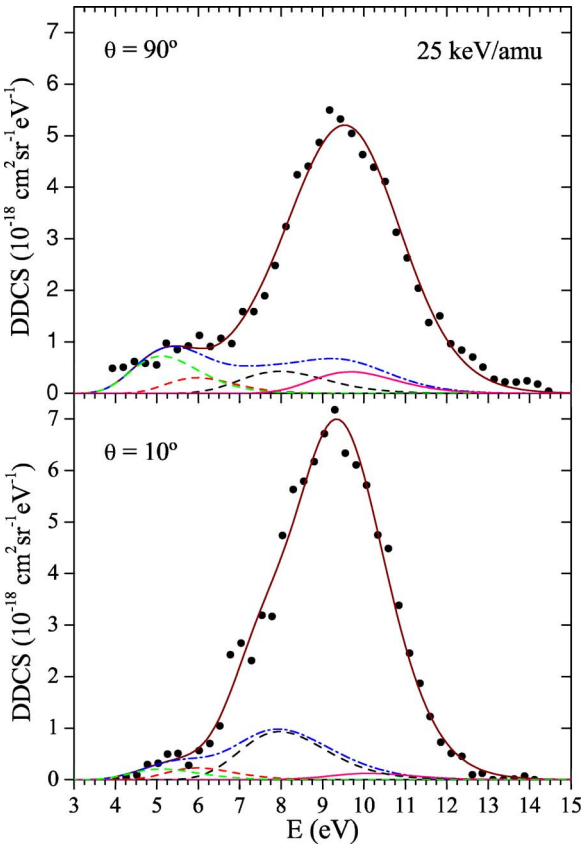

FIG. 7. (Color online) DDCS for proton emission in He^{2+} on H_2 at 25 keV/amu. (●) Total proton production; (·-·-·) ionization with excitation (IE) plus double ionization (DI); (- - -) ionization plus excitation (from lower to higher energies, $2p\pi_u$, $2s\sigma_g$, and $2p\sigma_u$ excited states); (—) double ionization.

tinuum (shake-off) states of the remaining one-electron target. In the so-called two-step mechanism, the two-electron transition results from the interaction of the projectile with each of the target electrons. As has been discussed in the literature [36], electron correlation can play a role in a two-step transition. Although, as a first approximation, the electrons can be considered independent. It has been established that a shake mechanism is dominant at high impact energy for two-electron processes (DI, TI) [11,33] where the sudden character of the collision prevents two successive projectile-electron interactions. At intermediate impact energies, when the collision time is long enough for two successive projectile-electron interactions, a dominant contribution from the two-step mechanism is expected [33]. It is worth noting that in a two-step picture both projectile-electron interactions may contribute to the orientation dependence of any two-electron process in H_2. In the case of the shake mechanism, the orientation dependence must be attributed to the single-electron transition produced by the projectile, while the promotion of the second electron will not contribute.

A two-step model calculation applied to the TE process was performed by Wang *et al.* [23] for H^+ on H_2, and by Corchs *et al.* [24] for O^{8+} on H_2. In the case of H^+ projectile at 1-MeV impact energy, they found that excitation shows a perpendicular orientation for the $2p\sigma_u$ state, and almost no angular dependence for the $2s\sigma_g$ and $2p\pi_u$ states. For O^{8+} on H_2, the theoretical results show that it is necessary to include the excitation step as well as the capture process to get a better agreement with experimental data. In the present results, experimental uncertainties do not allow us to distinguish a different angular pattern between the three dissociative excited states considered in TE and also in IE processes.

It may be interesting, however, to know the prediction of expression (1) for the single-electron capture process applied to the present measurements. Momentum transfer in the longitudinal direction for electron capture is given by $\alpha_z \simeq v_P/2 - Q/v_P$, where $Q=(E_f-E_i)$, with $E_i=-15.4$ eV and E_f, the initial and final electron binding energy, respectively [37]. At 25 keV/amu, capture to $He^+(2p)$ is the dominant channel. At 100 keV/amu mainly the $2p$ and $1s$ states are populated and, with decreasing probability, $2s$, $3p$, $3s$, and higher states [19,20]. From expression (1), the capture probability reads

$$|a_M(\mathbf{b})|^2 = |a_A(\mathbf{b}_A)|^2 + |a_B(\mathbf{b}_B)|^2 + 2\,\mathrm{Re}[a_A^*(\mathbf{b}_A)a_B(\mathbf{b}_B)e^{i\delta}]. \tag{4}$$

After integrating over impact parameter **b**, the first two terms result in twice the cross section for an atomic center. The orientation effect depends on the phase δ, as well as on the atomic probability amplitude. Constructive interference is obtained at θ=90°, and for other orientations in the range θ=0°–90°, depending on the value of $\alpha_z\rho$. Meanwhile, the product of atomic amplitudes favor the parallel orientation of the molecule (θ=0°, $\mathbf{b}_{A,B}=\mathbf{b}$). We applied to the present case

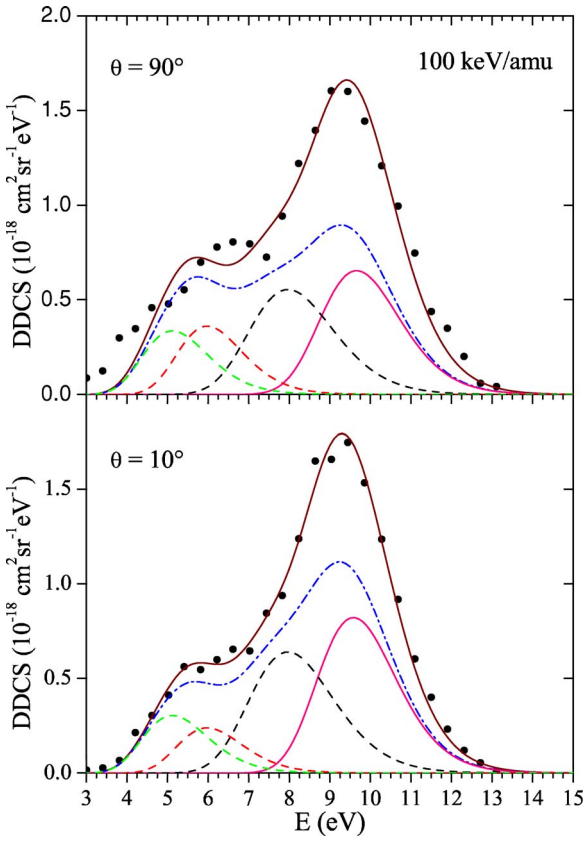

FIG. 8. (Color online) The same as in Fig. 7 for 100 keV/amu impact energy.

the formulation of Wang *et al.* [2,21] using the Brinkman-Kramers approximation in order to evaluate the atomic capture amplitude. The resulting single differential cross sections as a function of molecular orientation for capture to the relevant $n=2$ state at 25 keV/amu (capture to $n=1$ is also shown) and $n=1$, 2, and 3 at 100 keV/amu are shown in Fig. 12. At 100 keV/amu, the calculation predicts a perpendicular orientation in agreement with the experimental results obtained for TE, when the contributions for the three excited states ($2p\sigma_u$, $2s\sigma_g$, and $2p\pi_u$) are added; see Fig. 10. For 25 keV/amu the calculated distribution for transfer to the dominant $n=2$ state resulted in an isotropic behavior due to the compensation between the phase factor and the product of the atomic amplitudes. This is in contrast with the experimental result for the only relevant $2p\sigma_u$ state.

TABLE I. Single differential cross section $\sigma(\theta)=d\sigma/d(\cos\theta)$ for proton emission in He^{2+} on H_2 at 25 keV/amu. "Total dissociation" refers to the sum of dissociative processes resulting in proton emission. Cross section values are in 10^{-17} cm^2/rad units. $R=\sigma(10°)/\sigma(90°)$.

Process	σ (10°)	σ (90°)	R
Total dissociation	21.0±2.1	16.9±1.5	1.2±0.2
CE	8.6±0.6	8.6±0.4	1.0±0.1
DC	2.3±0.5	3.5±0.5	0.7±0.2
TE+TI	14.3±2.2	8.3±1.5	1.7±0.6
TI	6.1±0.8	4.1±0.7	1.5±0.4
TE ($2p\sigma_u$)	8.2±1.2	4.2±0.8	2.0±0.6
DI	<0.6	1.0±0.9	
IE	4.2±1.6	4.1±1.1	1.0±0.7
IE ($2p\sigma_u$)	3.1±1.4	1.4±0.9	
IE ($2s\sigma_g$)	0.6±0.5	0.8±0.5	
IE ($2p\pi_u$)	0.5±0.5	1.9±0.4	0.3±0.3

TABLE II. Same as in Table I for He^{2+} on H_2 at 100 keV/amu. Cross-section values are in 10^{-17} cm^2/rad units.

Process	σ (10°)	σ (90°)	R
Total dissociation	6.4±0.5	6.8±0.8	0.9±0.2
CE	2.2±0.1	2.1±0.1	1.0±0.1
DC	0.05±0.02	0.10±0.02	0.5±0.3
TE+TI	1.6±0.2	2.1±0.3	0.8±0.2
TI	0.9±0.1	1.0±0.1	0.9±0.2
TE	0.7±0.2	1.1±0.2	0.6±0.3
TE ($2p\sigma_u$)	0.41±0.12	0.77±0.12	0.5±0.2
TE ($2s\sigma_g$)	0.22±0.16	0.10±0.07	
TE ($2p\pi_u$)	0.05±0.04	0.20±0.08	<0.7
DI	1.3±0.2	1.0±0.2	1.2±0.4
IE	3.5±0.4	3.7±0.4	1.0±0.2
IE ($2p\sigma_u$)	2.1±0.2	1.8±0.2	1.2±0.3
IE ($2s\sigma_g$)	0.6±0.2	0.9±0.2	0.7±0.4
IE ($2p\pi_u$)	0.8±0.1	0.9±0.2	0.9±0.4

The model given by expression (1) can also be applied to IE, if it is assumed that the orientation dependence is determined by the ionization process. It must be noted that for electron capture the momentum transfer has an almost defined value, while there is a continuous distribution due to the different final states for the electron in the continuum for ionization. The change in the projectile momentum is in this case $\alpha_z \simeq (E_i - T)/v_P$, where T is the kinetic energy of the emitted electron. Cheng *et al.* [20] argued that integration over the final states washes out the interference pattern, and in fact they observed an isotropic behavior in the IE plus DI

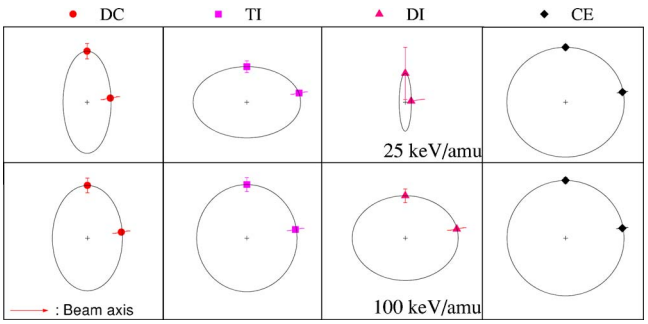

FIG. 9. (Color online) Molecular orientation (10° and 90°) relative to beam incidence direction for TI, DC, DI, and CE processes. The ellipse curves are drawn only to compare these two angles.

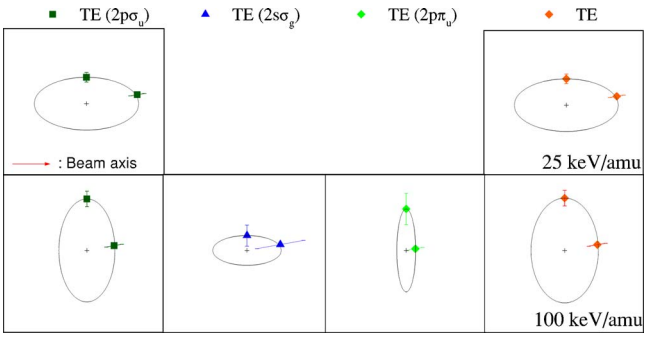

FIG. 10. (Color online) The same as in Fig. 9 for TE($2p\sigma_u$) and transfer plus excitation (TE) at 25 keV/amu and TE($2p\sigma_u$), TE($2s\sigma_g$), TE($2p\pi_u$) and the sum of these processes (TE) at 100 keV/amu.

spectra for O^{8+} on D_2 collisions. In the present case, if the contribution from the three excited states are added, an isotropic behavior is also observed for IE (Fig. 11). Regarding the double ionization process, an isotropic behavior should be expected as well, due to the contribution from the continuum distribution of kinetic energies in the final state. Again, at 100 keV/amu a small orientation effect is observed. At 25 keV/amu, the preference seems to be perpendicular, but the experimental uncertainties were large in the measured small contribution from this process.

Evidently, it is desirable to get a model calculation for two-electron processes, including the interference effect, with atomic transition amplitudes adequate at intermediate impact energies. Regardless of any specific model, in the case of a two-step mechanism in an independent electron approximation, the probability as a function of impact parameter can be written as the product of probabilities of the single-electron processes involved [15,23,35,36]. A simple model by Wohrer and Watson [38] makes use of the single-electron probability given by the expression $P(b) = P(0)\exp(-b/R)$, as it was applied by Dubois [39] for atomic targets. The parameter R is a typical interaction distance and $P(0)$ the probability at zero impact parameter. Then, the probability for the two-electron process reads

$$P_{1,2}(b) = P_1(0)\exp(-b_A/R_1)P_2(0)\exp(-b_B/R_2), \qquad (5)$$

where the projectile impact parameters $b_{A,B}$ with respect to the atomic centers A and B of the molecule are given by

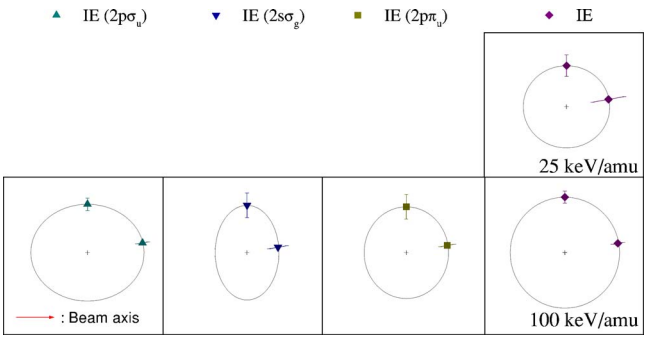

FIG. 11. (Color online) Same as in Fig. 9 for IE($2p\sigma_u$), IE($2p\pi_u$), and IE($2s\sigma_g$) at 100 keV/amu and the sum of these ionization plus excitation (IE) processes for 25 and 100 keV/amu.

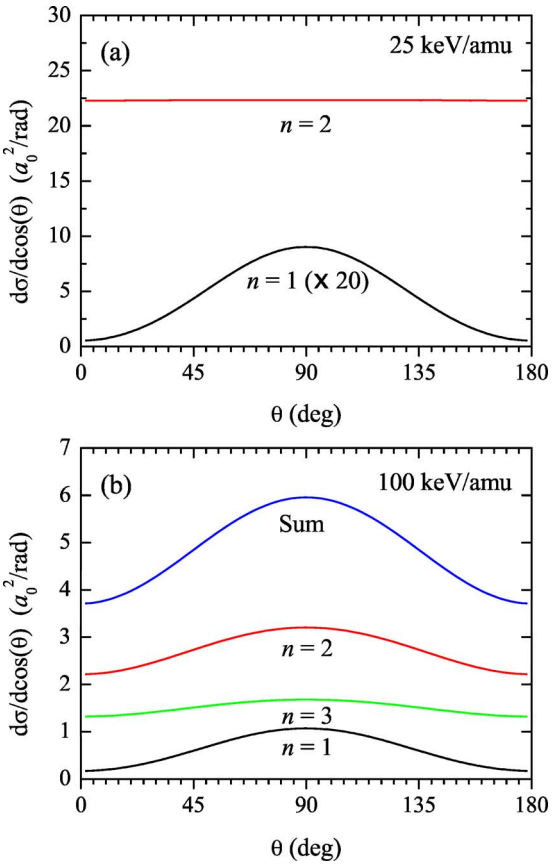

FIG. 12. (Color online) Angular differential cross section derived from Brinkman-Kramers model [2,21] for single capture in He^{2+} on H_2. (a) At 25 keV/amu. (b) At 100 keV/amu. The final He^+ electronic levels are indicated as n.

$$b_{A,B} = [b^2 + (\rho^2/4)\sin^2\theta \pm b\rho\sin\theta\cos\varphi]^{1/2}, \qquad (6)$$

with φ the angle within the collision plane and the plane containing the beam (z axis) and the internuclear $\boldsymbol{\rho}$ vector. After integration in angle φ and in impact parameter b, we obtained the probability $P_{1,2}(\theta)$ for the two-electron process as a function of molecular orientation, with the two interaction distances R_1 and R_2 as parameters. As we want only a qualitative picture based on this simple model, then $P_{1,2}(\theta)$ was evaluated at the following interaction distances $(R_1,R_2)=(\rho/2,\rho/2)$, $(\rho/2,\rho)$, (ρ,ρ) with $\rho=1.4$ a.u. If $P_{1,2}$ $(\theta=0°)$ are normalized to 1, the resulting angular distribution shows in all cases a maximum at $\theta=0°$, decreasing to values 0.5, 0.7, and 0.8 at $\theta=90°$ for increasing interaction distances. Therefore this model is not able to account for processes with a preferential perpendicular orientation, but illustrates the fact that the angular distribution approaches an isotropic distribution for increasing interaction distances.

If we now consider the TI process within a two-step mechanism of independent capture and ionization, capture has a higher probability than ionization at 25 keV/amu while ionization dominates at 100 keV/amu. However, as the TI probability results from the product of the probabilities of the corresponding single-electron process, any of the two processes or both will determine the orientation dependence for

TI. Fritsch [15] performed calculations on the orientation dependence for TI at low-energy $H^+ + H_2$ collisions. The probability of TI was modeled as the product of the probabilities of single capture and single ionization, which were determined within a close-coupling formalism. Calculations at 4-keV incident energy show a maximum for perpendicular orientation and a near isotropic behavior at 10 keV. These results were in agreement with experimental data from Yousif *et al.* [40], although these data include all the contributions to the CE channel. It was shown from calculations for the probabilities as a function of impact parameter that the observed results could be interpreted by means of the difference between the mean impact parameters for ionization and capture. Present results for the TI contribution to CE show that an orientation effect can be seen up to 25 keV/amu, while the isotropic behavior is reached at 100 keV/amu impact energy.

Returning now to the expression (1) based on a perburbative treatment, and again in a two-step independent electron approximation, it can be argued that ionization should not contribute to the orientation dependence, being the remaining transfer process the one that determines such a behavior. However, as was referred to above, the predicted isotropic behavior at 25 keV/amu and a pronounced perpendicular orientation at 100 keV/amu for capture is not observed in our TI results. Particularly, it is noticeable that the parallel orientation observed at 25 keV/amu is a trivial result only in a "geometric" model as presented above, expression (5).

Regarding the DC channel, it is the only two-electron process that shows the same orientation at both impact energies. At 25 keV/amu, it is known that mainly the $He(1s,2l)$ states are populated [41]. At 100 keV/amu, as our measurements did not include capture to doubly excited (autoionizing) states, only $He(1s,nl)$ final states must be taken into account. Considering a two-step transfer, we note that a one-electron transfer to $He^+(1s)$ must happen at both collision energies. Although some inconsistencies have been pointed out in application of the model given by expression (1) to a DC process viewed as a two-step process [2], it is interesting to note that a remarkable perpendicular orientation is obtained for the $He^+(1s)$ final state at both impact energies; see Fig. 12.

IV. CONCLUSIONS

We were able to measure the dependence on the molecular orientation of two-electron processes in dissociation of H_2 induced by He^{2+} projectiles. Particularly, this small energy range exhibits a transition from dominance of capture processes to a prevailing ionization. Furthermore, we observed a change with impact energy in the preferred orientation for some of the processes, which suggest it could serve as a severe test to model calculations. Since differential cross sections were obtained for proton emission only for two angles, the discussion was limited to perpendicular ($\theta=90°$), near parallel ($\theta=10°$), or isotropic angular behaviors.

The spectra analysis allowed us to separate the different contributions from the three main excited states in TE and IE. However, within the present uncertainties, we cannot assure that there is a difference in the orientation preference for each of these states. In the case of CE, we show that all the different processes leading to this final state, DC, TI, and DI, have different angular patterns, so they could be masked when only the total CE channel is considered.

Based on the assumption that the orientation effect is defined by the capture event, with small influence of the ionization and excitation steps, the observed results for DC, DI, TE, and IE at 100 keV/amu could be qualitatively interpreted by means of a perturbative model for the single capture process. TI probably requires a more detailed analysis about the dependence of the probabilities with impact parameter for the capture and ionization processes. At the impact energy of 25 keV/amu, the perturbative model for single capture is out of the range of validity. Taking into account the same assumption about the role of the capture in the determination of the alignment dependence, the parallel orientation observed for TI and TE would indicate the trend for the electron transfer to the expected He^+ ($n=2$) projectile final state. However, the double capture to the more probable $He(1s,2l)$) final state, with an observed perpendicular orientation, should be dominated by charge transfer to the $1s$ level. The present experimental results show that, even in a two-step formulation, it is necessary to have transition amplitudes for a single atomic center, with reliable dependence on the impact parameter, in order to predict the orientation preference of the molecule. Further experimental effort is required in order to establish the angular dependence for all the individual excited states ending up in dissociation.

ACKNOWLEDGMENTS

Support from the Consejo Nacional de Investigaciones Científicas y Técnicas (CONICET), the Agencia Nacional de Promoción Científica y Técnica (Contrato de Préstamo BID 1201/OC-AR, Grant No. 03-12567) and Fundación Antorchas are gratefully acknowledged.

[1] T. F. Tuan and E. Gerjuoy, Phys. Rev. **117**, 756 (1960).
[2] Y. D. Wang, J. H. McGuire, and R. D. Rivarola, Phys. Rev. A **40**, 3673 (1989).
[3] N. C. Deb, A. Jain, and J. H. McGuire, Phys. Rev. A **38**, 3769 (1988).
[4] S. E. Corchs, R. D. Rivarola, J. H. McGuire, and Y. D. Wang, Phys. Rev. A **47**, 201 (1993).
[5] H. F. Busnengo, S. E. Corchs, and R. D. Rivarola, Phys. Rev. A **57**, 2701 (1998).
[6] A. K. Edwards, R. M. Wood, and R. L. Ezell, Phys. Rev. A **31**, 99 (1985); **31**, 3972 (1985); **32**, 1873 (1985); **34**, 4411 (1986).

[7] D. Levesque and J. J. Weis, Phys. Rev. A **37**, 3697 (1988).
[8] A. K. Edwards, R. M. Wood, J. L. Davis, and R. L. Ezell, Phys. Rev. A **42**, 1367 (1990).
[9] A. K. Edwards, R. M. Wood, and R. L. Ezell, Phys. Rev. A **42**, 1799 (1990).
[10] L. Nagy and L. Végh, Phys. Rev. A **46**, 290 (1992).
[11] L. Nagy and L. Végh, Phys. Rev. A **50**, 3984 (1994).
[12] A. K. Edwards, R. M. Wood, M. A. Mangan, and R. L. Ezell, Phys. Rev. A **46**, 6970 (1992).
[13] R. Shingal and C. D. Lin, Phys. Rev. A **40**, 1302 (1989).
[14] W. Fritsch, Phys. Rev. A **46**, 3910 (1992).
[15] W. Fritsch, Phys. Lett. A **177**, 428 (1993).
[16] L. Meng, R. E. Olson, H. O. Folkerts, and R. Hoekstra, J. Phys. B **27**, 2269 (1994).
[17] M. B. Shah and H. B. Gilbody, J. Phys. B **11**, 121 (1978).
[18] G. F. Frieling, R. Hoekstra, E. Smulders, W. J. Dickson, A. N. Zinoviev, S. J. Kuppens, and F. J. de Heer, J. Phys. B **25**, 1245 (1992).
[19] R. Hoekstra, H. O. Folkerts, J. P. M. Beijers, R. Morgenstern, and F. J. de Heer, J. Phys. B **27**, 2021 (1994).
[20] S. Cheng, C. L. Cocke, V. Frohne, E. Y. Kamber, J. H. McGuire, and Y. Wang, Phys. Rev. A **47**, 3923 (1993).
[21] Y. D. Wang and J. H. McGuire, Phys. Rev. A **44**, 367 (1991).
[22] F. Busnengo, S. E. Corchs, R. D. Rivarola, and J. H. McGuire, Nucl. Instrum. Methods Phys. Res. B **98**, 227 (1995).
[23] Y. D. Wang, J. H. McGuire, O. L. Weaver, S. E. Corchs, and R. D. Rivarola, Phys. Rev. A **47**, 3966 (1993).
[24] S. E. Corchs, F. Busnengo, R. D. Rivarola, and J. H. McGuire, Nucl. Instrum. Methods Phys. Res. B **117**, 41 (1996).
[25] H. Braüning, I. Reiser, A. Diehl, A. Theiß, E. Sidky, C. L. Cocke, and E. Salzborn, J. Phys. B **34**, L321 (2001).
[26] I. Reiser, C. L. Cocke, and H. Braüning, Phys. Rev. A **67**, 062718 (2003).
[27] G. Bernardi, S. Suárez, D. Fregenal, P. Focke, and W. Meckbach, Rev. Sci. Instrum. **67**, 1761 (1996).
[28] S. Martínez, G. Bernardi, P. Focke, A. D. González, and S. Suárez, J. Phys. B **36**, 4813 (2003).
[29] P. Focke, G. Bernardi, D. Fregenal, R. O. Barrachina, and W. Meckbach, J. Phys. B **31**, 289 (1998).
[30] S. Martínez, G. Bernardi, P. Focke, A. D. González, and S. Suárez, J. Phys. B **35**, 2261 (2002).
[31] M. B. Shah, P. McCallion, and H. B. Gilbody, J. Phys. B **22**, 3983 (1989).
[32] M. B. Shah and H. B. Gilbody, J. Phys. B **15**, 3441 (1982).
[33] J. H. McGuire, Adv. At., Mol., Opt. Phys. **29**, 217 (1992).
[34] M. Kimura, Phys. Rev. A **32**, 802 (1985).
[35] K. M. Dunseath and D. S. F. Crothers, J. Phys. B **24**, 5003 (1991).
[36] J. H. McGuire, *Electron Correlation Dynamics in Atomic Collisions* (Cambridge University Press, Cambridge, England, 1997).
[37] M. R. C. McDowell and J. P. Coleman, *Introduction to the Theory of Ion-Atom Collisions* (North-Holland, Amstersdam, 1970).
[38] K. Wohrer and R. L. Watson, Phys. Rev. A **48**, 4784 (1993).
[39] R. D. DuBois, Phys. Rev. A **36**, 2585 (1987).
[40] F. B. Yousif, B. G. Lindsay, and C. J. Latimer, J. Phys. B **21**, 4157 (1988).
[41] L. F. Errea, A. Macías, L. Méndez, B. Pons, and A. Riera, J. Phys. B **36**, L135 (2003).